Desalination and Water Treatment
www.deswater.com
doi: 10.5004/dwt.2022.28661

268 (2022) 99–112
August

Adsorptive exclusion of crystal violet dye from wastewater using eggshells: kinetic and thermodynamic study

Sana Khadam[a], Tariq Javed[a,*], Muhammad Idrees Jilani[b]

[a]*Department of Chemistry, University of Sahiwal, Sahiwal, Pakistan, emails: mtariq@uosahiwal.edu.pk (T. Javed), sanakhadam13@gmail.com (S. Khadam)*
[b]*Department of chemistry, University of Lahore, Lahore, Pakistan, email: idreeschemistry@gmail.com*

Received 7 September 2021; Accepted 2 July 2022

ABSTRACT

The aim of current research was to remove methyl violet dye (MV) from wastewater by using eggshells. Batch experiments were performed to investigate the effect of different parameters, such as solution pH, adsorbent dose, contact time, dye concentration, and temperature, on adsorption of methyl violet dye. There was maximum, that is, 88% removal of methyl violet dye from wastewater at optimized conditions (i.e., pH 7, 0.6 g adsorbent dose, 10 min contact time, 40 ppm dye concentration, and 10°C temperature). Pseudo-first-order, pseudo-second-order, and intraparticle diffusion models were used to examine the adsorption process. Pseudo-second-order model was the best fit model for adsorption process with (R^2 = 0.9916). Adsorbent was characterized by scanning electron microscopy and Fourier transform infrared spectroscopy techniques. Adsorption isotherms such as Langmuir and Freundlich were studied and investigated. Langmuir isotherm model was best followed by adsorption process (R^2 = 0.9938). Thermodynamic parameters (i.e., ΔH, ΔG, and ΔS) were also investigated and results showed that process was spontaneous and exothermic. Applicability of developed practice with tap water was 82%.

Keywords: Methyl violet dye; Isotherms; Kinetic models; Thermodynamics; Eggshells

1. Introduction

In recent decades, environmental challenges caused by industrialization and urbanization have become more common and complex [1]. Dye are extensively employed in a variety of industries, with the textile industry being the greatest consumer and producer of dye-laden effluent [2]. Among various dyes, crystal/methyl violet is a synthetic cationic dye used for variety of purposes such as biological staining, dermatological agents, veterinary medicine, and additives to chicken feed in order to prevent mold, intestinal parasites, and to textile dyeing industries. It is a mutagen and a mitotic toxin, as well as a known carcinogen [3]. When it is ingested or inhaled it can induce cancer, gene mutations, allergies, and rashes [4], blepharospasm, gastrointestinal and respiratory tract irritation, nausea, abdominal pain, paralysis, peritonitis, weight loss, pulmonary edema, harmful reproductive effects, or birth defects, and cancer etc. [5]. It also triggers tumors and several eye itchiness and has been the most visible water-soluble class, an amount of less than 1.0 mg L^{-1} causes an evident coloration which inhibits photosynthetic activity [6]. The APVMA (Australian Pesticides and Veterinary Medicines Authority) of the NHMRC (National Health and Medical Research Council) disregarded the registration and pertinent approvals of the products containing methyl (crystal) violet after a 1994 special review of crystal (methyl) violet (APVMA 2014) [7].

Because an increasing number of hazardous organic and inorganic pollutants are found in water sources, one of today's global concerns is to provide healthy, pure water and

* Corresponding author.

to protect human health [8]. Dye removal from wastewater can be done in several different ways. Coagulation and flocculation, biological treatment, chemical oxidation, electrochemical treatment, ion exchange, and adsorption are some of the procedures used [9]. Among all, adsorption is the most appealing of these approaches for purification of dye-loaded effluents because it is simple, effective, environmentally acceptable, and cost-effective. Selection of an appropriate adsorbent, on the other hand, was always a difficult task [10]. To remove colors from aqueous solution, a range of low-cost adsorbents have been utilized, including clay materials, zeolites, siliceous materials, marine algae, chitosan, [11] bagasse pith, fuller's earth, and silica [12], wheat bran [13], spent tea leaves [14], orange peel [15], meranti saw dust [16], coconut bunch waste [17], mango seed [18], luffa acutangula peel [19] and many fish scale derivatives such as rohu (*Labeo rohita*) [20], piau (*Leporinus elongates*) scales [21] etc.

Eggshell is a common solid waste product in food processing and manufacturing plants. Because most eggshell trash has no practical utility, it is traditionally disposed of in landfills without being pretreated [22]. Eggshells are a calcium source found in nature [23]. Since eggshells were historically useless and were generally discarded in landfills without any pretreatment, substantial waste was from the egg-based product's processor [24]. Calcium, magnesium, and phosphorus are present in eggshell so eggshell has high nutritional value (Taco, 1982), this waste was commonly used as fertilizer, soil amendment, and or animal feed supplement (Christmas and Harms, 1976) [6]. Eggshell wastes have been used as a cement additive, a biodiesel catalyst, and a part of bone implants over the years. According to the study, waste eggshells were used as fertilizers (27%), animal feeds (21%), municipal dumps (26%), and several other restricted applications [25]. The eggshells that found their way to dumpsites can be used as an adsorbent to remove toxins from water. Activated carbon is commonly used to remove dyes, but it is expensive, and the recovery of used activated carbon is challenging. While, on the other hand, eggshell has a porous structure and pure calcium carbonate as the chief component. Due to high concentration of calcium carbonate, porous structure, and plenty of accessibility, toxic dyes can be removed from wastewater using eggshell waste as an adsorbent [26].

The aims of current research was to remove methyl violet dye from wastewater on eggshells by optimizing various adsorption parameters such as pH, adsorbent dose, contact time, dye concentration, and temperature, and to investigate isotherms, kinetics, and thermodynamics. Non-linear plots of isotherms have also been investigated.

2. Materials and methods

2.1. Collection of adsorbent

eggshells were collected from local bakery and washed with tap water followed by rinsing with distilled water. Eggshells were dried in sunlight for 4–5 d, grinned and sieved to get particles of different mesh sizes, that is, 500, 200, and 100 μm. Due to high porosity, adsorption percentage, and surface area of 100 μm sized particles, they were selected for further adsorption experiments.

2.2. Preparation of dye stock solution

1,000 ppm stock solution of methyl violet (MV) was prepared by dissolving 1 g of dye in a 1,000 mL measuring flask and diluting it with distilled water up to the mark. Fresh solutions were prepared for study of different parameters by diluting stock solution.

2.3. Batch adsorption studies

For optimization of different parameters such as pH, shaking time, adsorbent dose, dye concentration, and temperature, batch adsorption experiments were performed. Each experiment was carried out by keeping one parameter variable while other parameters remain constant. 10 mL of dye solution was used for each parameter study. For each parameter, adsorption solution was shaken and centrifuged for 3 min, filtered, followed by measuring absorbance of filtered solution by spectrophotometer. Percentage removal was calculated by equation given below:

$$\%\text{Removal} = \frac{C_o - C_e}{C_o} \times 100 \tag{1}$$

where C_o is initial dye concentration (mg L^{-1}) and C_e is equilibrium dye concentration (mg L^{-1}). adsorption capacity q_t (mg g^{-1}) can be obtained via following formulae:

$$q_t = \left(C_o - C_e\right) \times \frac{V}{m} \tag{2}$$

where V (mL) is volume of solution and m (g) is mass of adsorbent used [27,28].

3. Results and discussions

3.1. Characterization of adsorbent

Eggshells are characterized by Fourier transform infrared spectroscopy (FTIR; Perkin-Elmer Spectrum BX-II Model) and scanning electron microscopy (SEM; Model Hitachi S-3000N) functioning at 20 kV. FTIR was used to study that which functional groups of adsorbent were involved in adsorption of dye and SEM was used to study surface morphology of eggshells.

3.1.1. Fourier transform infrared spectroscopy

FTIR spectroscopy identifies different functional groups present on adsorbent surface [29,30] and gives information about kind of bonding involved in dye adsorption [28]. The stretching and bending vibrations of functional groups taking part in adsorption of adsorbate molecules were consequently measured using FTIR spectra of eggshells. Fig. 1 shows FTIR results of adsorbent both before and after dye adsorption. Before dye adsorption, FTIR spectral examination of adsorbent showed distinct peaks at 3,470; 2,929; 1,644; 1,160 and 650 cm^{-1}. Broad and strong band at 3,470 cm^{-1} confirmed the existence of –OH stretching. $–CH_2$ asymmetric stretching vibration is represented by band at 2,929 cm^{-1}. A prominent peak at 1,644 cm^{-1} can be attributed

to a –C=O stretching in carboxyl or amide groups. Carboxyl group show absorbance at 1,160 cm^{-1}. Characteristic band at 650 cm^{-1} is shown due to O–P–O bending vibrations of a phosphate group. After dye adsorption, maxima of –OH and –C=O stretching vibrations were moved from 3,470 and 1,644 cm^{-1} to 3,490 and 1,630 cm^{-1}, respectively. As a result, it's reasonable to assume that –OH and –C=O are primary adsorption sites for MV attachment on eggshell surfaces. Change in wavenumber of peak at 650 to 645 cm^{-1} indicates that MV interacts with $–PO_4$ functional group in eggshells. As a result, FTIR spectra suggest that functional groups on eggshell surface, such as –OH, –C=O, and $–PO_4$ are engaged in MV dye adsorption [22].

3.1.2. Scanning electron microscopy

Surface morphology and texture of eggshell powder was examined using scanning electron microscopy both before and after adsorption. Macroporous structure and highly irregular surface of powdered eggshell can be seen in images (Figs. 2 and 3) taken at a magnification of 2,000 X. Furthermore, excessive porosity of eggshell powder particles is also shown in Fig. 2, which might be pointed out as gas-exchange pores. Before dye adsorption (Fig. 2), adsorbent surface was highly porous and rough which after dye uptake (Fig. 3) became smoother and homogenous [8].

3.2. Effect of pH

Series of batch adsorption studies were performed over a pH range of 1–12 to examine the effect of solution pH on adsorption of MV by eggshells. Results (Fig. 4 and Table S1) showed that percentage of dye removal increased with increase in pH of dye solution, reaching a maximum at neutral pH, that is, 7.0. with further increase in pH, no significant change in dye removal was found. Hence, for next experiments, optimum pH 7.0 was selected. Surface charge of biosorbent and degree of ionization of dye molecule are affected by solution pH. Protonation of functional groups, present on surface of eggshells such as –OH, –C=O, and $–PO_4$, at low pH levels imparts the adsorbent surface a net positive charge, whereas deprotonation at high pH levels gives it a net negative charge resulting in greater amount of dye removal. MV has a pKa of 8; at pH greater than 8, it is completely ionized and exists as cationic species. Positively charged dye ions and positively charged adsorbent surface have a considerable electrostatic repulsion at low pH levels, as a result, dye removal was minimal. Due to strong electrostatic attraction between negatively charged sites on adsorbent and cationic dye molecules (at higher/basic pH levels) a significant increase in adsorption percentage was found. Reduction of H^+ ions, which challenge dye cations for specific locations on adsorbent surface at lower pH, may also account for increase in dye removal capability at higher pH. This competition lessens when pH rises, and dye cations replace H^+ ions linked

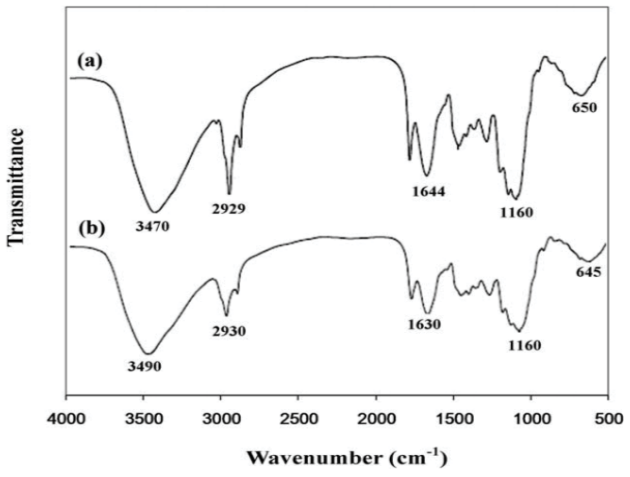

Fig. 1. FTIR spectrum of eggshells (a) before adsorption and (b) after adsorption [22].

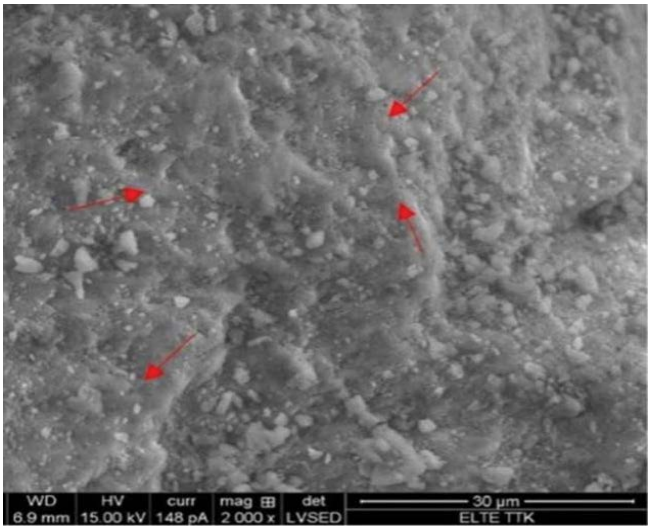

Fig. 2. SEM results before crystal violet dye adsorption on eggshells [8].

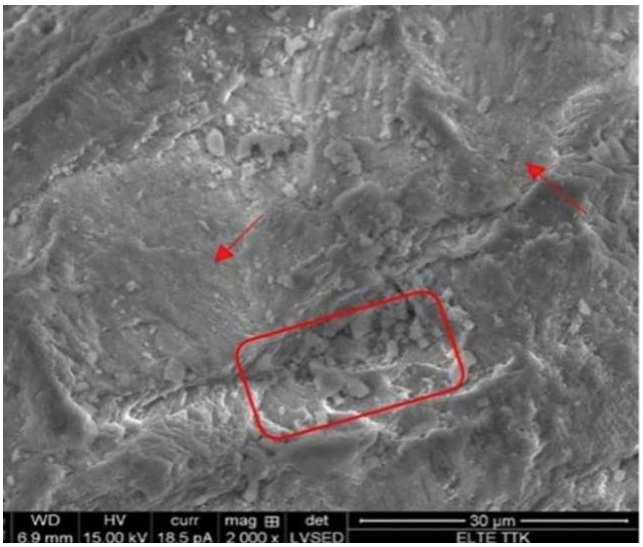

Fig. 3. SEM results after crystal violet dye adsorption on eggshells [8].

to the adsorbent surface, leading to higher dye uptake. Similar results have been reported by [31].

3.3. Effect of adsorbent dose

Effect of adsorbent amount for dye removal was examined in range of 0.1–1 g (Fig. 5 and Table S2). As the adsorbent amount is increased from 0.1 to 0.6 g, percentage of dye removal also increased due to increase in adsorptive surface area and availability of more active/adsorption sites which are primarily responsible for this development [32–34]. Equilibrium adsorption capacity, on the other hand, reduces as the amount of adsorbent increases. This could be because of overlapping or clumping of adsorption sites which reduced the total adsorption surface area available to dye molecules. As adsorbent mass increased, amount of dye adsorbed on unit mass of adsorbent decreases, resulting in a drop in % removal of dye as adsorbent mass concentration increased. The maximum dye removal was observed at 0.6 g, and increasing the adsorbent dosage does not increase the adsorption yield considerably. Because nearly all dye molecules adhere to adsorbent surface and an equilibrium was established between dye molecules on adsorbent and in the solution. Similar results have been reported by [33,34].

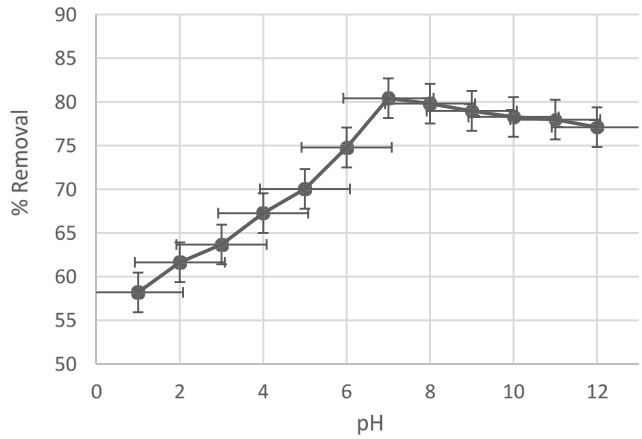

Fig. 4. Effect of solution pH on adsorption of methyl violet dye on eggshells.

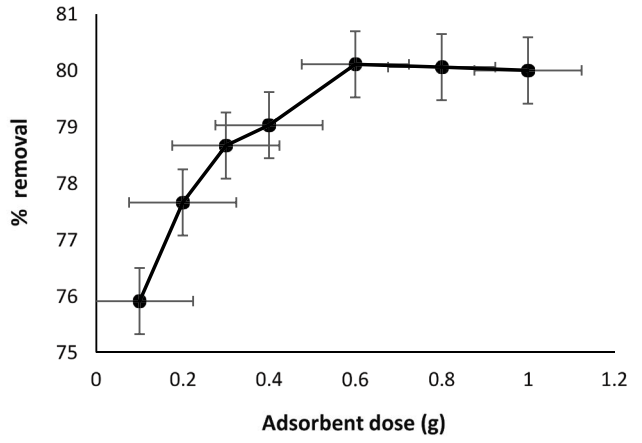

Fig. 5. Effect of adsorbent dose on adsorption of methyl violet dye by eggshells.

3.4. Effect of contact time

Effect of contact time on adsorption of methyl violet by eggshells was examined by varying time from 5–120 min. Results (Fig. 6 and Table S3) showed that maximum adsorption occurred within 10 min after which there was a decrease in adsorption efficiency. Fast reaction in beginning was due to presence of vacant adsorption spots at exterior of adsorbent. After some time, all the vacant sites were occupied by dye molecules resulting in less increase in dye abstraction because at saturation point dye molecules are weakly held on adsorbent surface (probably known as second adsorption layer) [35,36]. In other words at saturation point active sites of adsorbent were impregnated with dye molecules [37].

3.5. Effect of dye concentration

Adsorption efficiency of eggshells at various initial methyl violet concentrations, that is, 5–120 ppm was investigated. Results (Fig. 7 and Table S4) showed that percentage removal increased continuously from 5–40 ppm dye concentration after which there was a decrease in percentage removal because at saturation point all active sites of adsorbent were impregnated with dye molecules. Besides repulsion between dye molecules also takes place responsible for decrease in percentage removal of dye [38,39].

3.6. Effect of temperature

To optimize temperature parameter, solution temperature varied from 10°C–60°C. Results of experiment (Fig. 8 and Table S5) showed that crystal violet (CV) dye removal using eggshells decreased with increase in temperature

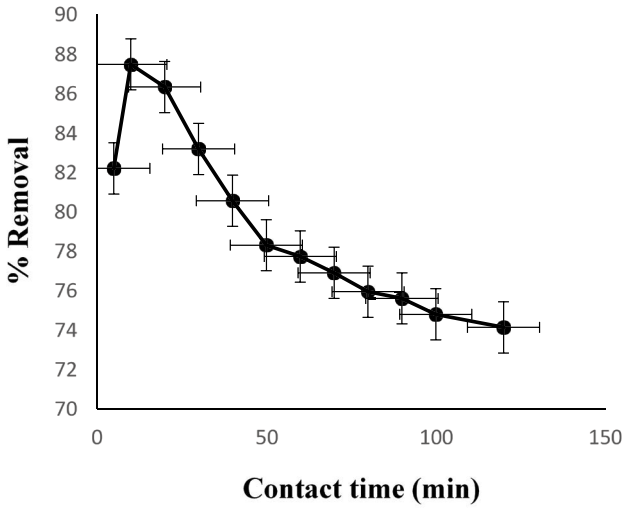

Fig. 6. Effect of contact time on adsorption of methyl violet dye by eggshells.

showing that the process of crystal violet (CV) dye adsorption on eggshells was of exothermic kind since at elevated temperature, bonds between dye and adsorbent's binding sites weaken, that is, adsorbate-solvent interactions overcome adsorbate–adsorbent interactions leading to decrease in removal percentage of dye. Hence, process found to be exothermic in nature [40–44].

3.7. Adsorption kinetic models

Effectiveness of an adsorbent is determined by kinetics of adsorption [45]. This describes various elements that influence rate of a chemical reaction. Adsorption of methyl violet dye by eggshells was analyzed by three models as pseudo-first-order, pseudo-second-order, and intraparticle diffusion model.

According to pseudo-first-order kinetic model, "rate of adsorption has direct relation with number of available active/adsorption sites." Linear form of pseudo-first-order reaction is as:

$$\ln\left(q_e - q_t\right) = \ln q_e - K_f t \tag{3}$$

where q_t (mg g^{-1}) is amount of dye adsorbed on adsorbent surface at time t, q_e (mg g^{-1}) is amount of dye adsorbed on adsorbent exterior at equilibrium time, K_f is pseudo-first-order constant. By plotting a graph between $\ln(q_e - q_t)$ and time t (min) we get a straight line graph. K_f and q_e can be obtained from slope and intercept of this graph [46]. Results of experiment and graph given in Table S6 and Fig. 9. Results showed that R^2 value for pseudo-first-order kinetic model was 0.9742 (less than 1). Additionally, there was greater difference amongst calculated, that is, 8.3×10^{-4} mg g^{-1} and experimental, that is, 0.198 mg g^{-1} q_e values showing that current adsorption process does not follow pseudo-first-order kinetic model.

Pseudo-second-order model shows that chemisorption is involved in process [47]. Linear form of pseudo-second-order model is given below:

$$\frac{t}{q_t} = \frac{1}{K_s q_e^2} + \frac{t}{q_e} \tag{4}$$

where q_t (mg g^{-1}) = amount of adsorbate adsorbed on adsorbent surface at time t, q_e (mg g^{-1}) = amount of adsorbate adsorbed on adsorbent surface at equilibrium time, and K_s (g mg^{-1} min^{-1}) = pseudo-second-order rate constant. A straight-line graph (shown in Fig. 10 and statistical data in Table S7) was obtained when we plot t/q_t (min g mg^{-1}) vs. time (min) from which slope and intercept can be determined [46]. Higher R^2 value of pseudo-second-order model confirmed that it is the best fitted model for adsorption of methyl violet dye by eggshells. Similar trend was observed with various adsorbents [48–50].

To check the rate-controlling step, intraparticle diffusion model was investigated on adsorption of methyl violet by eggshells. Intraparticle diffusion model equation is as follows:

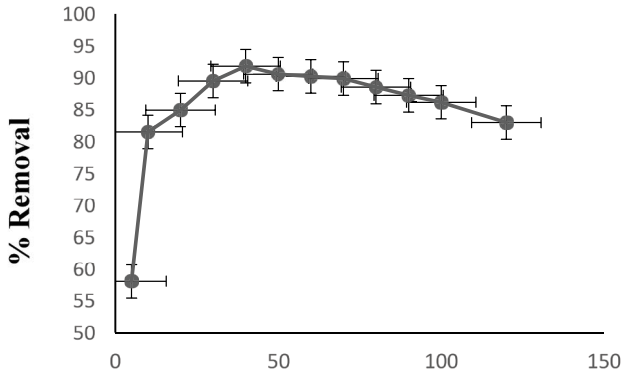

Fig. 7. Effect of dye concentration on adsorption of methyl violet dye by eggshells.

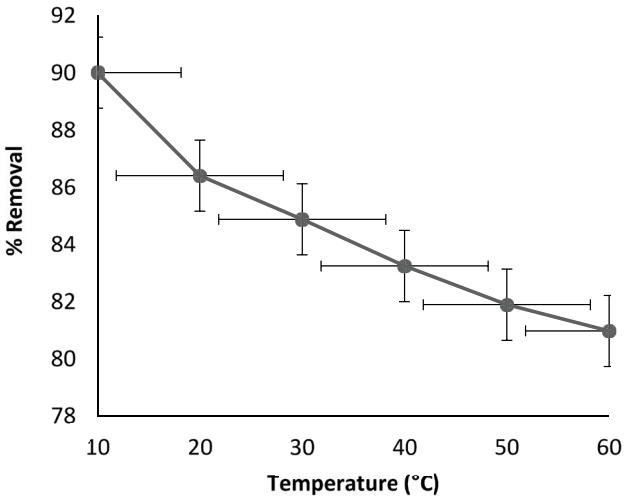

Fig. 8. Effect of temperature on adsorption of methyl violet dye by eggshells.

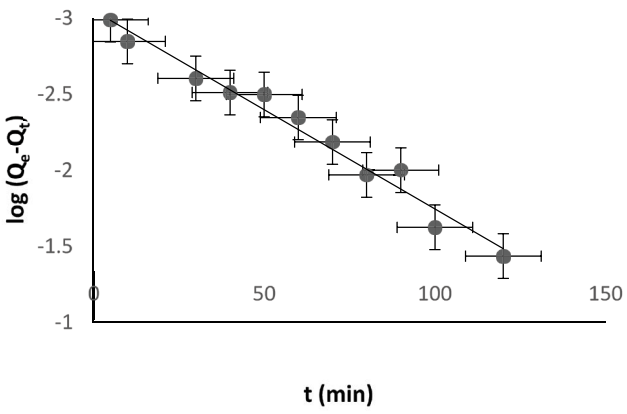

Fig. 9. Plot of pseudo-first-order model for adsorption of methyl violet dye by eggshells.

$$q_t = K_{id} t^{0.5} + I \quad (5)$$

where q_t (mg g^{-1}) = quantity of adsorbate adsorbed at time 't', I = thickness of layer and K_{id} (mg g^{-1} min^{-1}) = intraparticle diffusion constant [48]. Plot obtained by data is not linear (shown in Fig. 11 and statistical data in Table S8). It means that only intra particle diffusion model is not the rate limiting step, but other kinetic models are also involved in control of adsorption speed [48]. Comparison of kinetic parameters of three models is given in Table 1.

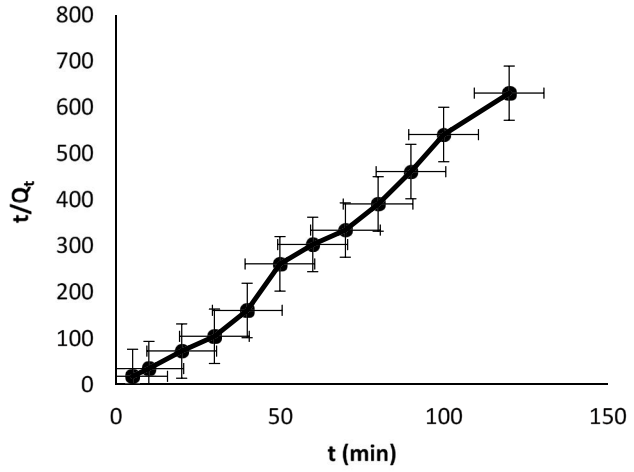

Fig. 10. Plot of pseudo-second-order model for adsorption of methyl violet dye on eggshells.

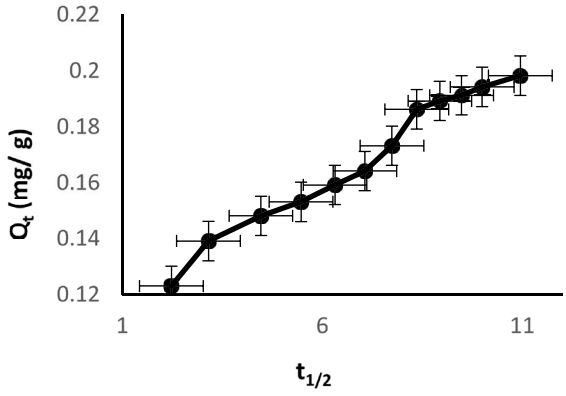

Fig. 11. Plot of intraparticle diffusion model for adsorption of methyl violet dye by eggshells.

3.8. Adsorption isotherm models

Different isotherm models, that is, Langmuir, Freundlich, and Dubinin–Radushkevich (D–R) isotherm models, were used to evaluate concentration data from experiment of crystal violet dye adsorption on eggshells. These isotherms provide insight for relationship between adsorbate concentration in solution and amount of dye adsorbed on adsorbent surface [51].

According to Langmuir isotherm model, adsorption occurs at specified homogenous locations on adsorbent surface [52]. It deals with monolayer adsorption. Linear form of Langmuir model is as follows:

$$\frac{1}{q_e} = \frac{1}{q_{max}} + \left(\frac{1}{q_{max} K_L}\right)\frac{1}{C_e} \text{ [53]} \quad (6)$$

where K_L = Langmuir constant (dm^{-3} mol^{-1}) and q_{max} = monolayer adsorption capacity (mg g^{-1}). This equation can be written simply as:

$$\frac{C_e}{q_e} = \frac{1}{q_{max} K_L} + \left(\frac{C_e}{q_{max}}\right) \quad (7)$$

When we plot a graph between C_e (mg L^{-1})/q_e (mg g^{-1}) vs. C_e (mg L^{-1}), then a straight line was obtained [46]. Separation factor (R_L) was used to investigate whether the process is favorable or unfavorable. Process is favorable only when $0 < R_L < 1$ while it is unfavorable when $R_L > 1$ and linear for $R_L = 1$ and irreversible for $R_L = 0$. Formula of R_L is as follows:

$$R_L = \frac{1}{1 + bC_{In}} \quad (8)$$

where b = Langmuir adsorption equilibrium constant (L mol^{-1}), C_{In} = initial dye concentration (L mol^{-1}). From b and C_{In} we can determine R_L [48]. Results (Table S9) showed that process of adsorption was linear in nature (confirmed by R_L = 1). Statistical results of Langmuir adsorption isotherm (Table S10 and Fig. 12) showed that R^2 value of this model was 0. 9928 (close to unity) showing that data was the best fit to Langmuir isotherm model. Non-linear plot of Langmuir isotherm model is given in Fig. S1.

Freundlich isotherm is an empirical equation used to explain the adsorption process on heterogeneous surfaces. Linear form of Freundlich adsorption isotherm model is:

$$\ln q_e = K_F + \frac{1}{n}\ln P \quad (9)$$

Table 1
Comparison of kinetic parameters of three models, that is, pseudo-first-order, pseudo-second-order, and intraparticle diffusion model

Pseudo-first-order kinetic model	Pseudo-second-order kinetic model	Intraparticle diffusion kinetic model
Experimental q_e = 0.198 mg g^{-1}	Experimental q_e = 0.198 mg g^{-1}	Experimental q_e = 0.198 mg g^{-1}
Calculated $q_e = 8.3 \times 10^{-4}$ mg g^{-1}	Calculated q_e = 0.197 mg g^{-1}	Calculated q_e = 0.107 mg g^{-1}
R^2 = 0.9742	R^2 = 0.9918	R^2 = 0.9773
K_1 (min^{-1}) = 0.03086	K_2 (min^{-1}) = 0.7537	K_{id} (min^{-1}) = 0.0087

In case of solution, this equation can take form as:

$$\ln q_e = K_f + \frac{1}{n}\ln C_e \tag{10}$$

where K_f = Freundlich constant, n = slope, q_e (mg g^{-1}) = amount of dye adsorbed per gram of an adsorbent. By plotting $\ln q_e$ vs. $\ln C_e$ a straight line graph (Fig. 13 and Table S11) was obtained. From intercept and slope of graph "K_f" and "n" can be calculated [46]. R^2 value for Freundlich isotherm model was 0.9757, that is, less than that of Langmuir adsorption isotherm model which confirmed that statistical data follows Langmuir isotherm model. Non-linear plot of Freundlich isotherm model is given in Fig. S2.

Dubinin–Radushkevich isotherm model is an empirical model that explains mechanism of adsorption with a Gaussian surface distribution on a heterogeneous surface. This model has a semi-empirical equation that follows pore filling mechanism [54]. Equation for Dubinin–Radushkevich is as:

$$\ln q_e = \ln q_{\mathrm{DR}} - \beta\varepsilon^2 \tag{11}$$

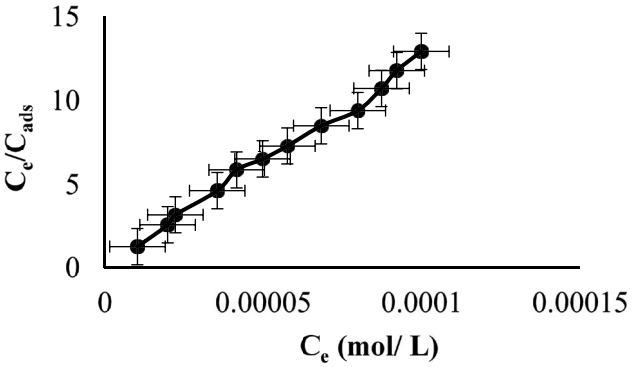

Fig. 12. Langmuir isotherm plot for methyl violet dye adsorption by eggshells.

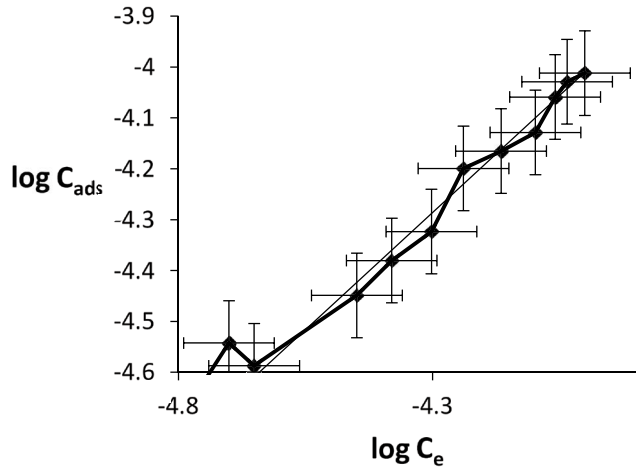

Fig. 13. Freundlich isotherm plot for adsorption of methyl violet dye by eggshells.

where β = activity coefficient, $\ln q_{\mathrm{DR}}$ = imaginary inundation capacity, ε is Polanyi potential as follows:

$$\varepsilon = RT\ln\left(1+\frac{1}{C_e}\right) \tag{12}$$

where T = temperature, R is general gas constant. Energy of transference of one mole of solute from infinity to adsorbent surface is mean sorption energy denoted by β.

$$\beta = \frac{1}{\sqrt{2\beta}} \tag{13}$$

where β = activity coefficient [46]. Results of experiments and graph for D–R isotherm was given in Table S12 and Fig. 14 and non-linear graph was shown in Fig. S3. Value of R^2 for D–R isotherm model is 0.9443 which is less than that of Freundlich adsorption isotherm model and value of energy (calculated from D–R isotherm model) indicated the process to be chemical as well physical in its kind.

On comparing results of different isotherm models (Table 2), we found that data fits the best to Langmuir isotherm model rather than Freundlich and D–R isotherm models since R^2 value of Langmuir isotherm model is very close to unity as compared to other models. Comparison of adsorption capacities of different adsorbents for methyl violet dye exclusion is given in Table 3.

3.9. Thermodynamics of adsorption

Effect of temperature on adsorption of methyl violet dye is an important parameter that determines whether the process was exothermic or endothermic [61]. Equation used to calculate thermodynamic parameters is as:

$$K_c = \frac{C_{\mathrm{ads}}}{C_{\mathrm{eq}}} \tag{14}$$

where C_{ads} (mg L^{-1}) = amount of dye adsorbed on surface of adsorbent at equilibrium while C_{eq} (mg L^{-1}) = amount of dye

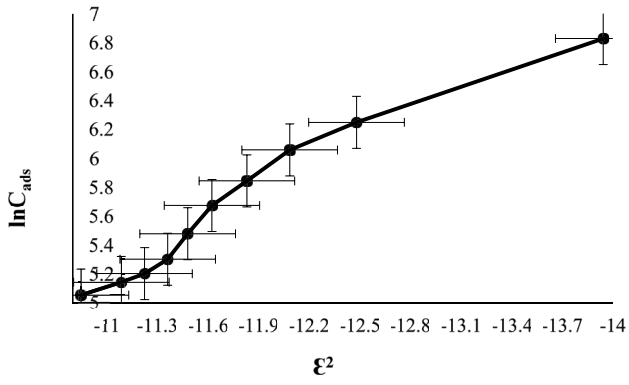

Fig. 14. D–R isotherm plot for adsorption of methyl violet dye on eggshells.

Table 2
Comparison of isotherm models parameters, that is, Langmuir, Freundlich and Dubinin–Radushkevich model

Langmuir isotherm model	Q_o (mg g^{-1}) = 1.08E-08	b (dm^3 mol^{-1}) = 8.6E-06	R^2 = 0.9928
Freundlich isotherm model	K_f (mg g^{-1}) = 1.80E+03	n (L g^{-1}) = 0.21	R^2 = 0.9757
Dubinin–Radushkevich isotherm model	$\beta = Q_o$ (kJ^2 mol^{-2}) = 0.6188	ε^2 (kJ mol^{-1}) = 2	R^2 = 0.9443

Table 3
Comparison of adsorption capacities of different adsorbents for methyl violet dye exclusion

Adsorbent	Adsorption capacity (mg g^{-1})	References
Eggshell	25.73	Present study
Ground nutshell	0.524	[55]
Bean pod	0.380	[55]
MWCNTs/$MnO_8ZnO_2Fe_2O_4$ nanoparticles	5.00	[56]
Keratin nanoparticles	1.57	[57]
Coniferous pinus bark	0.72	[58]
Breadfruit	6.88	[59]
Activated carbon	18.47	[60]

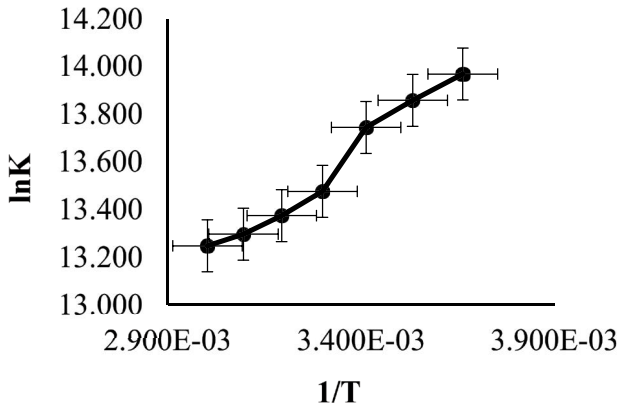

Fig. 15. Van't Hoff plot of methyl violet dye adsorption by eggshells.

remaining in solution at equilibrium. Van't Hoff equation relates ΔH and ΔS with K_c by the following equation:

$$\ln K_c = -\frac{\Delta H}{RT} + \frac{\Delta S}{R} \quad (15)$$

where R is the universal gas constant = 8.31 J mol^{-1} K^{-1} and T = temperature in Kelvin. A straight-line graph was obtained by plotting $\ln K_c$ against $1/T$ from which ΔH and ΔS can be determined. Equation which relates Gibb's free energy with enthalpy and entropy is as:

$$\Delta G = \Delta H - T\Delta S \text{ [62]} \quad (16)$$

Van't Hoff plot is shown in Fig. 15. Statistical data for thermodynamic parameters is given in Table S13. Negative

Table 4
Calculated thermodynamic parameters

ΔG (kJ mol^{-1})	ΔH (kJ mol^{-1})	ΔS (kJ mol^{-1})
–31.017	9.723	0.149
–31.857	9.723	0.147
–32.755	9.723	0.145
–33.210	9.723	0.142
–34.047	9.723	0.140
–34.931	9.723	0.138
–35.878	9.723	0.137

Table 5
Results of regeneration study

Adsorbent	Eggshells
Adsorbate	Crystal violet
Desorbing agent used	HNO3
Contact time	10 min
% age removal	78%

ΔG value confirmed the process to be spontaneous in nature and randomness of process increased as confirmed by positive ΔS. Positive value of enthalpy change determine that process is of endothermic nature [63–65] as given in Table 4.

3.10. Desorption study

Regeneration of adsorbent is an important parameter in determining the proficiency and effectivity of adsorbent used [34,66]. Nitric acid solution (1 M HNO_3) was used for desorption of methyl/crystal violet dye. For this 0.6 g of dye loaded coconut husk (adsorbent) was shaken with 1 molar nitric acid solution for 10 min to recover both adsorbent and adsorbate. Results (Table 5) showed that nearly 78% of desorption takes place. Yet, removal efficacy of adsorbent decreased after regeneration but can be reused for treatment [37,48,62,67–69].

3.11. Applicability of developed process with tap water

Applicability of procedure with a real system was investigated by treating the adsorbent with tap water [48] providing optimized conditions (i.e., solution pH of 7.0, 0.6 adsorbent dose, 10 min contact time, 40 mg L^{-1} dye concentration, and 0°C temperature). Results showed that nearly 82% of methyl violet removal was take place confirming the applicability of developed practice with real samples (results are shown in Table 6).

Table 6
Results of developed procedure with tap water

Adsorbent	Eggshells
Adsorbate	Methyl violet
Water used	Tap water instead of distilled water
Percentage removal	82%

4. Conclusion

Eggshell works as an effective adsorbent to remove methyl violet dye from wastewater. Maximum adsorption occurs at pH 7.0, 0.6 adsorbent dose, 10 min contact time, 40 ppm dye concentration, and 10°C temperature resulting in 88% removal of methyl violet dye. Adsorption of methyl violet by eggshells followed pseudo-second-order kinetics. FTIR was used for functional groups analysis and to investigate which functional groups are involved in adsorption process. SEM was used to study surface morphology of eggshells. Langmuir isotherm best fitted to adsorption of methyl violet dye by eggshells. Thermodynamic study revealed that the process was endothermic and spontaneous. Desorption study showed that eggshells are recyclable and hence are effective and efficient adsorbent for wastewater treatment.

Conflicts of interest

Authors state no competing financial concerns to influence the work described in this research.

Availability of data and material (data transparency)

Authors will ensure data transparency.

Authors' contributions

All authors contribute equally to the manuscript.

Data availability

The data that support this study are available in the article and accompanying supplementary file.

References

[1] A. Babuponnusami, S. Velmurugan, Investigation on adsorption of dye (Reactive Red 35) on egg shell powder, Int. J. ChemTech Res., 10 (2017) 565–572.
[2] R. Slimani, I. El Ouahabi, S. Benkaddour, H. Hiyane, M. Essoufy, Y. Achour, S. El Antri, S. Lazar, M. El Haddad, Removal efficiency of textile dyes from aqueous solutions using calcined waste of eggshells as eco-friendly adsorbent: kinetic and thermodynamic studies, Chem. Biochem. Eng. Q., 35 (2021) 43–56.
[3] G. Crini, E. Lichtfouse, Advantages and disadvantages of techniques used for wastewater treatment, Environ. Chem. Lett., 17 (2019) 145–155.
[4] D. Kim, Y. Kim, J.H. Choi, K.S. Ryoo, Evaluation of natural and calcined eggshell as adsorbent for phosphorous removal from water, Bull. Korean Chem. Soc., 41 (2020) 650–656.
[5] S.B. Martínez, J. Pérez-Parra, R. Suay, Use of ozone in wastewater treatment to produce water suitable for irrigation, Water Resour. Manage., 25 (2011) 2109–2124.
[6] H. Daraei, A. Mittal, J. Mittal, H. Kamali, Optimization of Cr(VI) removal onto biosorbent eggshell membrane: experimental & theoretical approaches, Desal. Water Treat., 52 (2014) 1307–1315.
[7] M. Sun, K. Ricker, G. Osborne, M. Marder, R. Schmitz, Evidence on the Carcinogenicity of Gentian Violet, Office of Enviromental Health Hazard Assessment (OEHHA), 2018, pp. 11–14.
[8] E. Rápó, L.E. Aradi, Á. Szabó, K. Posta, R. Szép, S. Tonk, Adsorption of Remazol Brilliant Violet-5R textile dye from aqueous solutions by using eggshell waste biosorbent, Sci. Rep., 10 (2020) 1–12.
[9] A.R. Yari, G. Majidi, M.T. Reshvanloo, S. Nazari, M. Emami Kale Sar, M. Khazaei, M.S. Tabatabai-Majd, Using eggshell in acid orange 2 dye removal from aqueous solution, Iran. J. Health Sci., 3 (2015) 38–45.
[10] F. Mashkoor, A. Nasar, A.M. Asiri, Exploring the reusability of synthetically contaminated wastewater containing crystal violet dye using *Tectona grandis* sawdust as a very low-cost adsorbent, Sci. Rep., 8 (2018) 1–16.
[11] A. Borhade, A. Kale, Calcined eggshell as a cost effective material for removal of dyes from aqueous solution, Appl. Water Sci., 7 (2017) 4255–4268.
[12] S. Allen, Types of Adsorbent Materials, CRC Press, Boca Raton, FL, 1996.
[13] M. Sulak, E. Demirbas, M. Kobya, Removal of Astrazon Yellow 7GL from aqueous solutions by adsorption onto wheat bran, Bioresour. Technol., 98 (2007) 2590–2598.
[14] N. Nasuha, B. Hameed, A.T.M. Din, Rejected tea as a potential low-cost adsorbent for the removal of methylene blue, J. Hazard. Mater., 175 (2010) 126–132.
[15] M. Arami, N.Y. Limaee, N.M. Mahmoodi, N.S. Tabrizi, Removal of dyes from colored textile wastewater by orange peel adsorbent: equilibrium and kinetic studies, J. Colloid Interface Sci., 288 (2005) 371–376.
[16] A. Ahmad, M. Rafatullah, O. Sulaiman, M. Ibrahim, R. Hashim, Scavenging behaviour of meranti sawdust in the removal of methylene blue from aqueous solution, J. Hazard. Mater., 170 (2009) 357–365.
[17] B. Hameed, D. Mahmoud, A. Ahmad, Equilibrium modeling and kinetic studies on the adsorption of basic dye by a low-cost adsorbent: coconut (*Cocos nucifera*) bunch waste, J. Hazard. Mater., 158 (2008) 65–72.
[18] W.S. Alencar, E. Acayanka, E.C. Lima, B. Royer, F.E. De Souza, J. Lameira, C.N. Alves, Application of *Mangifera indica* (mango) seeds as a biosorbent for removal of Victazol Orange 3R dye from aqueous solution and study of the biosorption mechanism, Chem. Eng. J., 209 (2012) 577–588.
[19] H.W. Ng, L.Y. Lee, W.L. Chan, S. Gan, N. Chemmangattuvalappil, *Luffa acutangula* peel as an effective natural biosorbent for malachite green removal in aqueous media: equilibrium, kinetic and thermodynamic investigations, Desal. Water Treat., 57 (16) (2016) 7302–7311.
[20] S. Chowdhury, P. Das Saha, U. Ghosh, Fish (*Labeo rohita*) scales as potential low-cost biosorbent for removal of malachite green from aqueous solutions, Biorem. J., 16 (2012) 235–242.
[21] E.F. Vieira, A.R. Cestari, W.A. Carvalho, C. Dos S. Oliveira, R.A. Chagas, The use of freshwater fish scale of the species *Leporinus elongatus* as adsorbent for anionic dyes: an isothermal calorimetric study, J. Therm. Anal. Calorim., 109 (2012) 1407–1412.
[22] S. Chowdhury, P. Das, Utilization of a domestic waste—eggshells for removal of hazardous malachite green from aqueous solutions, Environ. Prog. Sustainable Energy, 31 (2012) 415–425.
[23] K. Workeneh, E.A. Zereffa, T.A. Segne, R. Eswaramoorthy, Eggshell-derived nanohydroxyapatite adsorbent for defluoridation of drinking water from bofo of Ethiopia, J. Nanomater., 2019 (2019) 2458312, doi: 10.1155/2019/2458312.
[24] B. Haddad, A. Mittal, J. Mittal, A. Paolone, D. Villemin, M. Debdab, G. Mimanne, A. Habibi, Z. Hamidi, M. Boumediene, Synthesis and characterization of egg shell (ES) and egg shell with membrane (ESM) modified by ionic liquids, Chem. Data Collect., 33 (2021) 100717, doi: 10.1016/j.cdc.2021.100717.

[25] A. Mariyam, J. Mittal, F. Sakina, R.T. Baker, A.K. Sharma, A. Mittal, Efficient batch and fixed-bed sequestration of a basic dye using a novel variant of ordered mesoporous carbon as adsorbent, Arabian J. Chem., 14 (2021) 103186, doi: 10.1016/j.arabjc.2021.103186.
[26] S. Soni, P. Bajpai, J. Mittal, C. Arora, Utilisation of cobalt doped iron based MOF for enhanced removal and recovery of methylene blue dye from waste water, J. Mol. Liq., 314 (2020) 113642, doi: 10.1016/j.molliq.2020.113642.
[27] S. Chowdhury, S. Chakraborty, P.D. Saha, Removal of crystal violet from aqueous solution by adsorption onto eggshells: equilibrium, kinetics, thermodynamics and artificial neural network modeling, Waste Biomass Valorization, 4 (2013) 655–664.
[28] A. Bukhari, T. Javed, M.N. Haider, Adsorptive exclusion of crystal violet dye from wastewater by using fish scales as an adsorbent, J. Dispersion Sci. Technol., (2022) 1–12, doi: 10.1080/01932691.2022.2059506.
[29] S. Chakraborty, A. Mukherjee, S. Das, N. Raju Maddela, S. Iram, P. Das, Study on isotherm, kinetics, and thermodynamics of adsorption of crystal violet dye by calcium oxide modified fly ash, Environ. Eng. Res., 26 (2020), doi: 10.4491/eer.2019.372.
[30] M. Abbas, Z. Harrache, M. Trari, Mass-transfer processes in the adsorption of crystal violet by activated carbon derived from pomegranate peels: kinetics and thermodynamic studies, J. Eng. Fibers Fabr., 15 (2020), doi: 10.1177%2F1558925020919847.
[31] P. Balamurugan, G. Vinnilavu, Removal of methyl violet dye from industrial waste water using neem leaf powder, Indian J. Ecol., 47 (2020) 442–445.
[32] K. Karthik, B. Sudhkar, P.S. Pranav, V. Sridevi, Removal of crystal violet dye from aqueous solution through biosorption using *Lysiloma latisilinquum* seed powder: kinetics and isotherm, Int. J. Eng. Res. Tech., 8 (2019) 493–497.
[33] D. Sujata, S. Shalini, G. Shashank, Evaluation of wheat bran as a biosorbent for potential mitigation of dye pollution in industrial wastewaters, Orient. J. Chem., 35 (2019) 1565–1573.
[34] Z.U. Zango, S.S. Imam, Evaluation of microcrystalline cellulose from groundnut shell for the removal of crystal violet and methylene blue, Nanosci. Nanotechnol., 8 (2018) 1–6.
[35] N.J. Okorocha, C.E. Omaliko, C.C. Osuagwu, M.O. Chijioke-Okere, C.K. Enenebeaku, Utilization of agro-waste in the elimination of dyes from aqueous solution: equilibrium, kinetic and thermodynamic studies, Int. Lett. Chem. Phys. Astron., 86 (2021) 11–23.
[36] W.C. Wanyonyi, J.M. Onyari, P.M. Shiundu, Adsorption of Congo red dye from aqueous solutions using roots of *Eichhornia crassipes*: kinetic and equilibrium studies, Energy Procedia, 50 (2014) 862–869.
[37] S. Sultana, K. Islam, M.A. Hasan, H.J. Khan, M.A.R. Khan, A. Deb, M. Al Raihan, M.W. Rahman, Adsorption of crystal violet dye by coconut husk powder: isotherm, kinetics and thermodynamics perspectives, Environ. Nanotechnol. Monit. Manage., (2022) 100651, doi: 10.1016/j.enmm.2022.100651.
[38] T. Nargawe, A.K. Rai, R. Ameta, S.C. Ameta, Adsorption study for removal of crystal violet dye using MMT-MWCNTS composite from aqueous solution, J. Appl. Chem., 7 (2018) 1252–1259.
[39] A. Kant, P. Gaijon, U. Nadeem, Adsorption equilibrium and kinetics of crystal violet dye from aqueous media onto waste material, Chem. Sci. Rev. Lett., 3 (2014) 1–13.
[40] M. Alshabanat, G. Alsenani, R. Almufarij, Removal of crystal violet dye from aqueous solutions onto date palm fiber by adsorption technique, J. Chem., 2013 (2013), doi: 10.1155/2013/210239.
[41] T.C. Chandra, M. Mirna, Y. Sudaryanto, S. Ismadji, Adsorption of basic dye onto activated carbon prepared from durian shell: studies of adsorption equilibrium and kinetics, Chem. Eng. J., 127 (2007) 121–129.
[42] G.K. Cheruiyot, W.C. Wanyonyi, J.J. Kiplimo, E.N. Maina, Adsorption of toxic crystal violet dye using coffee husks: equilibrium, kinetics and thermodynamics study, Sci. Afr., 5 (2019) e00116, doi: 10.1016/j.sciaf.2019.e00116.
[43] Y.-S. Ho, T.-H. Chiang, Y.-M. Hsueh, Removal of basic dye from aqueous solution using tree fern as a biosorbent, Process Biochem., 40 (2005) 119–124.
[44] S. Shoukat, H.N. Bhatti, M. Iqbal, S. Noreen, Mango stone biocomposite preparation and application for crystal violet adsorption: a mechanistic study, Microporous Mesoporous Mater., 239 (2017) 180–189.
[45] D.F. Romdhane, Y. Satlaoui, R. Nasraoui, A. Charef, R. Azouzi, Adsorption, modeling, thermodynamic, and kinetic studies of methyl red removal from textile-polluted water using natural and purified organic matter rich clays as low-cost adsorbent, J. Chem., 2020 (2020), doi: 10.1155/2020/4376173.
[46] K. Hayat, Studies on Sorption of Methylene Blue Over *Cedrus deodara* saw, Vol. 2017, p. 97.
[47] V.M. Alamillo-López, V. Sánchez-Mendieta, O.F. Olea-Mejía, M.G. González-Pedroza, R.A. Morales-Luckie, Efficient removal of heavy metals from aqueous solutions using a bionanocomposite of eggshell/Ag-Fe, Catalysts, 10 (2020) 727, doi: 10.3390/catal10070727.
[48] M. Batool, T. Javed, M. Wasim, S. Zafar, M.I. Din, Exploring the usability of *Cedrus deodara* sawdust for decontamination of wastewater containing crystal violet dye, Desal. Water Treat., 224 (2021) 433–448.
[49] H. Patel, R. Vashi, Adsorption of crystal violet dye onto tamarind seed powder, E-J. Chem., 7 (2010) 975–984.
[50] B. Singh, B. Walia, R. Arora, Parametric and kinetic study for the adsorption of crystal violet dye by using carbonized eucalyptus, Int. J. Comput. Eng. Res., 8 (2018) 1–11.
[51] M.T. Yagub, T.K. Sen, S. Afroze, H.M. Ang, Dye and its removal from aqueous solution by adsorption: a review, Adv. Colloid Interface Sci., 209 (2014) 172–184.
[52] A. Murcia-Salvador, J.A. Pellicer, M.I. Rodríguez-López, V.M. Gómez-López, E. Núñez-Delicado, J.A. Gabaldón, Egg by-products as a tool to remove direct blue 78 dye from wastewater: kinetic, equilibrium modeling, thermodynamics and desorption properties, Materials, 13 (2020) 1262, doi: 10.3390/ma13061262.
[53] A. Wathukarage, I. Herath, M. Iqbal, M. Vithanage, Mechanistic understanding of crystal violet dye sorption by woody biochar: implications for wastewater treatment, Environ. Geochem. Health, 41 (2019) 1647–1661.
[54] S. Kaur, S. Rani, R.K. Mahajan, Adsorption of dye crystal violet onto surface-modified *Eichhornia crassipes*, Desal. Water Treat., 53 (2015) 1957–1969.
[55] L. Akinola, A. Umar, Adsorption of crystal violet onto adsorbents derived from agricultural wastes: kinetic and equilibrium studies, J. Appl. Sci. Environ. Manage., 19 (2015) 279–288.
[56] M. Gabal, E. Al-Harthy, Y. Al Angari, M.A. Salam, MWCNTs decorated with $Mn_{0.8}Zn_{0.2}Fe_2O_4$ nanoparticles for removal of crystal-violet dye from aqueous solutions, Chem. Eng. J., 255 (2014) 156–164.
[57] F. Abbasi, M.T. Yaraki, A. Farrokhnia, M. Bamdad, Keratin nanoparticles obtained from human hair for removal of crystal violet from aqueous solution: optimized by Taguchi method, Int. J. Biol. Macromol., 143 (2020) 492–500.
[58] R. Ahmad, Studies on adsorption of crystal violet dye from aqueous solution onto coniferous Pinus bark powder (CPBP), J. Hazard. Mater., 171 (2009) 767–773.
[59] L.B. Lim, N. Priyantha, N.H.M. Mansor, *Artocarpus altilis* (breadfruit) skin as a potential low-cost biosorbent for the removal of crystal violet dye: equilibrium, thermodynamics and kinetics studies, Environ. Earth Sci., 73 (2015) 3239–3247.
[60] T. Aysu, M. Küçük, Removal of crystal violet and methylene blue from aqueous solutions by activated carbon prepared from *Ferula orientalis*, Int. J. Environ. Sci. Technol., 12 (2015) 2273–2284.
[61] M. Sulyman, M. Sienkiewicz, J. Haponiuk, S. Zalewski, New approach for adsorptive removal of oil in wastewater using textile fibers as alternative adsorbent, Acta Sci. Agric., 2 (2018) 1–6.
[62] J. Tariq, K. Nasir, M.L. Mirza, Kinetics, equilibrium and thermodynamics of cerium removal by adsorption on low-rank coal, Desal. Water Treat., 89 (2017) 240–249.
[63] M. Ertaş, B. Acemioğlu, M.H. Alma, M. Usta, Removal of methylene blue from aqueous solution using cotton stalk, cotton waste and cotton dust, J. Hazard. Mater., 183 (2010) 421–427.

[64] S. Hong, C. Wen, J. He, F. Gan, Y.-S. Ho, Adsorption thermodynamics of methylene blue onto bentonite, J. Hazard. Mater., 167 (2009) 630–633.
[65] O.J. Nnaemeka, O.J. Josphine, O. Charles, Adsorption of basic and acidic dyes onto agricultural wastes, Int. Lett. Chem. Phys. Astron., 70 (2016) 13, doi: 10.18052/www.scipress.com/ILCPA.70.12.
[66] P.V. Nidheesh, R. Gandhimathi, S.T. Ramesh, T.S.A. Singh, Adsorption and desorption characteristics of crystal violet in bottom ash column, J. Urban Environ. Eng., 6 (2012) 18–29.
[67] P. Sun, C. Hui, R. Azim Khan, J. Du, Q. Zhang, Y.-H. Zhao, Efficient removal of Crystal violet using Fe_3O_4-coated biochar: the role of the Fe_3O_4 nanoparticles and modeling study their adsorption behavior, Sci. Rep., 5 (2015) 1–12.
[68] M. Abbaz, The removal and desorption of two toxic dyes from aqueous solution by hydroxylated hematite sand: kinetics and equilibrium, J. Appl. Chem. Environ. Prot., 2 (2017) 305–314.
[69] N. Bagotia, A.K. Sharma, S. Kumar, A review on modified sugarcane bagasse biosorbent for removal of dyes, Chemosphere, 268 (2021) 129309, doi: 10.1016/j.chemosphere.2020.129309.

Supporting information

Table S1
Results of experiment to study the effects of solution pH

pH	C_e	% adsorption
1	2.3467	58.19
2	2.5067	61.63
3	2.64	63.67
4	2.44	67.26
5	2.2533	70.03
6	2	74.78
7	1.0267	80.41
8	1.36	79.8
9	1.6267	78.96
10	17,867	78.28
11	1.76	77.96
12	1.16	77.1

Table S2
Results of experiment to study the effects of adsorbent dosage

Adsorbent dosage (g)	C_e	% adsorption
0.1	2.2133	75.91
0.2	2.04	77.66
0.4	1.9333	78.67
0.6	1.8933	79.03
0.8	1.7867	80.11
1.0	1.7733	80.06

Table S3
Results of experiment to study the effect of contact time

Time (min)	C_e	% adsorption
5	1.44	82.203
10	1.0133	87.48
20	0.9733	86.33
30	1.36	83.19
40	2.5067	80.56
50	1.5333	78.3
60	2.5067	77.73
70	1.6267	76.9
80	1.9467	75.94
90	1.9733	75.6
100	2.04	74.79

Table S4
Results of experiment to study the effects of dye concentration

Dye concentration (ppm)	C_e	% adsorption
5	4.2356	58.06
10	3.609	81.49
20	4.6366	84.93
30	4.2607	89.5
40	3.7093	91.81
50	4.411	90.57
60	4.6867	90.21
70	4.8872	89.88
80	5.4387	88.53
90	6.0652	87.23
100	6.5915	86.15
120	8.1203	82.97

Table S5
Results of experiment to study the effects of temperature

Temperature (°C)	C_e	% adsorption
10	4.787	89.6
20	5.3634	86.4
30	7.0175	84.87
40	7.7694	83.24
50	8.3961	81.89
60	8.8221	80.97

Table S6
Investigational statistics for pseudo-first-order kinetics

Time (min)	C_e (mg L^{-1})	q_t (mg g^{-1})	$q_e - q_t$	$\log(q_e - q_t)$
5	1.44	0.123	0.1779	–2.987
10	1.0133	0.139	0.16189	–2.845
20	0.9733	0.148	0.15289	
30	1.36	0.153	0.148	–2.602
40	2.5067	0.16	0.1418	–2.509
50	1.5333	0.1640	0.1369	–2.496
60	2.5067	0.173	0.12789	–2.345
70	1.6267	0.186	0.11489	–2.184
80	1.9467	0.189	0.11189	–1.968
90	1.9733	0.191	0.10989	–1.852
100	2.04	0.194	0.10689	–1.624
120	2.0933	0.198	0.10289	–1.435

Table S7
Investigational statistics for pseudo-second-order kinetics

Time (min)	C_e (mg L^{-1})	q_t (mg g^{-1})	t/q_t
5	1.44	0.123	17.24
10	1.0133	0.139	34.352
20	0.9733	0.148	72.256
30	1.36	0.153	104.167
40	2.5067	0.16	160.143
50	1.5333	0.1640	200.356
60	2.5067	0.173	250.285
70	1.6267	0.186	333.789
80	1.9467	0.189	390.423
90	1.9733	0.191	460.425
100	2.04	0.194	540.587
120	2.0933	0.198	630.214

Table S8
Investigational statistics for intraparticle diffusion model

Time (min)	C_e (mg L^{-1})	q_t (mg g^{-1})	$t^{1/2}$
5	1.44	0.123	2.23607
10	1.0133	0.139	3.16228
20	0.9733	0.148	4.47214
30	1.36	0.153	5.47723
40	2.5067	0.16	6.32456
50	1.5333	0.1640	7.07107
60	2.5067	0.173	7.74597
70	1.6267	0.186	8.3666
80	1.9467	0.189	8.94427
90	1.9733	0.191	9.48683
100	2.04	0.194	10
120	2.0933	0.198	10.9545

Table S9
Calculations for R_L values

b	Initial dye concentration (mol L^{-1})	R_L
8.5749×10^{-7}	1.22555E-05	1.000000236
8.5749×10^{-7}	2.45111E-05	1.000000471
8.5749×10^{-7}	4.90221E-05	1.000000943
8.5749×10^{-7}	7.35332E-05	1.000001414
8.5749×10^{-7}	9.80443E-05	1.000001886
8.5749×10^{-7}	0.000122555	1.000002357
8.5749×10^{-7}	0.000147066	1.000002828
8.5749×10^{-7}	0.000171577	1.0000033
8.5749×10^{-7}	0.000196089	1.000003771
8.5749×10^{-7}	0.0002206	1.000004243
8.5749×10^{-7}	0.000245111	1.000004714
8.5749×10^{-7}	0.000294133	1.000005657

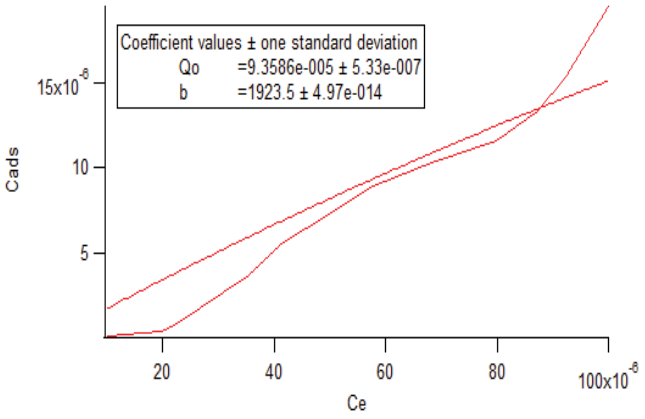

Fig. S1. Non-linear plot of Langmuir isotherm model.

Table S10
Experimental data for Langmuir isotherm model

C_o (mg L^{-1})	C_o (mol L^{-1})	C_e (mg L^{-1})	C_e (mol L^{-1})	C_{ads} (mol g^{-1})	C_e/C_{ads} (g L^{-1})
5	1.22555E-05	4.2356	1.02E-05	2.01553E-07	1.987
10	2.45111E-05	3.609	1.99E-05	4.58107E-07	2.754
20	4.90221E-05	4.6366	2.23E-05	8.8051E-07	4.658
30	7.35332E-05	4.2607	3.56E-05	3.79632E-06	5.984
40	9.80443E-05	3.7093	4.17E-05	5.63943E-06	7.124
50	0.000122555	4.411	4.99E-05	7.26853E-06	8.625
60	0.000147066	4.6867	5.77E-05	8.94164E-06	9.487
70	0.000171577	4.8872	6.83E-05	1.03237E-05	11.254
80	0.000196089	5.4387	7.99E-05	1.16239E-05	12.987
90	0.0002206	6.0652	8.73E-05	1.3328E-05	14.584
100	0.000245111	6.5915	9.22E-05	1.52941E-05	15.547
120	0.000294133	8.1203	9.99E-05	1.94263E-05	15.999

Table S11
Experimental data for Freundlich isotherm model

C_o (mg L^{-1})	C_o (mol L^{-1})	C_e (mg L^{-1})	C_e (mol L^{-1})	logC_e	logC_{ads}
5	1.22555E-05	4.2356	1.02E-05	–4.989700043	–4.9897
10	2.45111E-05	3.609	1.99E-05	–4.700492701	–4.5424
20	4.90221E-05	4.6366	2.23E-05	–4.650916831	–4.5871
30	7.35332E-05	4.2607	3.56E-05	–4.448916135	–4.4489
40	9.80443E-05	3.7093	4.17E-05	–4.380384994	–4.3804
50	0.000122555	4.411	4.99E-05	–4.302160632	–4.3235
60	0.000147066	4.6867	5.77E-05	–4.239200688	–4.1992
70	0.000171577	4.8872	6.83E-05	–4.165325026	–4.1653
80	0.000196089	5.4387	7.99E-05	–4.09772508	–4.1287
90	0.0002206	6.0652	8.73E-05	–4.058886273	–4.0589
100	0.000245111	6.5915	9.22E-05	–4.035410413	–4.029
120	0.000294133	8.1203	9.99E-05	–4.00056495	–4.0119

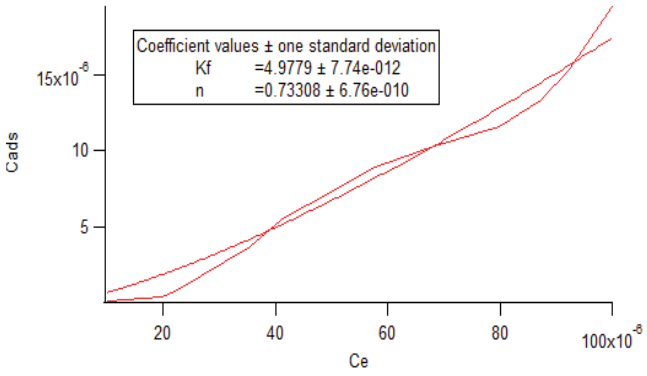

Fig. S2. Non-linear plot of Freundlich isotherm model.

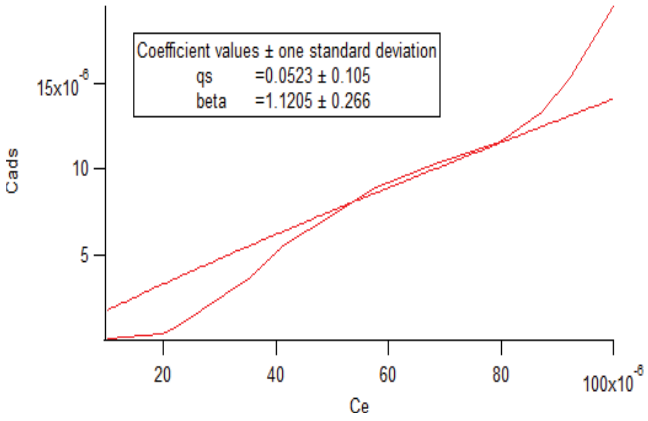

Fig. S3. Non-linear plot of D–R isotherm model.

Table S12
Experimental data for Dubinin–Radushkevich model

C_o (mg L^{-1})	C_e (mol L^{-1})	C_{ads} (mol g^{-1})	lnC_{ads}	ε	ε^2
5	1.02E-05	2.01553E-07	–15.4172120	2.803599264	0.684134292
10	1.99E-05	4.58107E-07	–14.5961640	2.641102728	6.975423622
20	2.23E-05	8.8051E-07	–13.9427641	2.613247784	6.829063983
30	3.56E-05	3.79632E-06	–12.4814784	2.499751505	6.248757587
40	4.17E-05	5.63943E-06	–12.0857282	2.46124693	6.057736448
50	4.99E-05	7.26853E-06	–11.8319561	2.41729648	5.843322271
60	5.77E-05	8.94164E-06	–11.6247916	2.381922646	5.67355549
70	6.83E-05	1.03237E-05	–11.4810638	2.340416232	5.477548139
80	7.99E-05	1.16239E-05	–11.3624513	2.302436198	5.301212447
90	8.73E-05	1.3328E-05	–11.2256465	2.280615396	5.201206584
100	9.22E-05	1.52941E-05	–11.0880456	2.267426038	5.141220836
120	9.99E-05	1.94263E-05	–10.8488838	2.247849059	5.052825392

Table S13
Investigational statistics for thermodynamic parameters

C_e (mg L^{-1})	C_e (mol L^{-1})	C_a (mol L^{-1})	T (°C)	T (K)	$1/T$	K_c	$\ln K_c$
4.2857	1.050E-05	1.223E+01	0	273	3.663E-03	1164611.1	13.968
4.787	1.173E-05	1.223E+01	10	283	3.534E-03	1042651.6	13.857
5.3634	1.315E-05	1.223E+01	20	293	3.413E-03	930598.68	13.744
7.0175	1.720E-05	1.223E+01	30	303	3.300E-03	711246.36	13.475
7.7694	1.904E-05	1.223E+01	40	313	3.195E-03	642413.90	13.373
8.3961	2.058E-05	1.223E+01	50	323	3.096E-03	594462.90	13.295
8.8221	2.162E-05	1.223E+01	60	333	3.003E-03	565757.53	13.246